Endothelial cells use dynamic actin to facilitate lymphocyte transendothelial migration and maintain the monolayer barrier

Olivia L. Mooren, Jinmei Li, Julie Nawas, and John A. Cooper
Department of Cell Biology and Physiology, Washington University, St. Louis, MO 63110

ABSTRACT **The vascular endothelium is a highly dynamic structure, and the integrity of its barrier function is tightly regulated. Normally impenetrable to cells, the endothelium actively assists lymphocytes to exit the bloodstream during inflammation. The actin cytoskeleton of the endothelial cell (EC) is known to facilitate transmigration, but the cellular and molecular mechanisms are not well understood. Here we report that actin assembly in the EC, induced by Arp2/3 complex under control of WAVE2, is important for several steps in the process of transmigration. To begin transmigration, ECs deploy actin-based membrane protrusions that create a cup-shaped docking structure for the lymphocyte. We found that docking structure formation involves the localization and activation of Arp2/3 complex by WAVE2. The next step in transmigration is creation of a migratory pore, and we found that endothelial WAVE2 is needed for lymphocytes to follow a transcellular route through an EC. Later, ECs use actin-based protrusions to close the gap behind the lymphocyte, which we discovered is also driven by WAVE2. Finally, we found that ECs in resting endothelial monolayers use lamellipodial protrusions dependent on WAVE2 to form and maintain contacts and junctions between cells.**

Monitoring Editor
Thomas D. Pollard
Yale University

Received: May 14, 2014
Revised: Oct 10, 2014
Accepted: Oct 14, 2014

INTRODUCTION

Endothelial cells (ECs) have critical roles in the immune and vascular systems. First, they establish and maintain the barrier between the blood stream and the underlying tissues. Second, they facilitate the migration of leukocytes from the blood into the tissue. Both functions are highly dynamic and regulated. During inflammation, the barrier opens in a regulated manner to allow for the passage of fluids, cytokines, and leukocytes. Dysfunction of the endothelial barrier is a prominent component of many disease states, including atherosclerosis, chronic inflammation, and diabetes (Weber *et al.*, 2007; Dejana *et al.*, 2008; Bakker *et al.*, 2009; Kumar *et al.*, 2009; Sima *et al.*, 2009; Rigor *et al.*, 2013).

Transendothelial migration (TEM), or diapedesis, is the process by which leukocytes cross from the bloodstream into the underlying tissue. ECs actively participate in this process, interacting with the migrating leukocytes in a complex network of cross-signaling between the cells (Wittchen, 2009; Nourshargh *et al.*, 2010). Signaling networks in both cells orchestrate complex dynamic changes in the actin cytoskeleton (Barreiro *et al.*, 2004; Nourshargh *et al.*, 2010), which control the shape of the cells and generate the forces that move the leukocyte across the endothelium. The molecular mechanisms for movement by leukocytes have been relatively well studied, but much less is known about the mechanisms by which ECs enable and promote leukocyte transmigration.

The first step in TEM is formation of a protrusive docking structure on the surface of the EC, which cups the leukocytes. The second step is formation of a transmigratory pore, either within one EC (the "transcellular" route) or between two ECs (the "paracellular" route). The final step is closure of the pore after the leukocytes completely transits across the monolayer.

For the paracellular migration route, leukocytes bind to cell junction proteins, such as PECAM, CD99, and JAMs (Muller *et al.*, 1993; Ostermann *et al.*, 2002; Schenkel *et al.*, 2002; Bradfield *et al.*, 2007; Lou *et al.*, 2007; Sircar *et al.*, 2007; Weber *et al.*, 2007), and they

This article was published online ahead of print in MBoC in Press (http://www.molbiolcell.org/cgi/doi/10.1091/mbc.E14-05-0976) on October 29, 2014.

Address correspondence to: John Cooper (jcooper@wustl.edu).

Abbreviations used: EC, endothelial cell; EGTA, ethylene glycol tetraacetic acid; LatA, latrunculin A; PBL, peripheral blood lymphocyte; TEM, transendothelial migration; TER, transendothelial resistance.

move through loosened cell–cell junctions. In the transcellular migration route, leukocytes pass through a transcellular channel created by the EC. Transcellular migration involves integrin-based interactions between the leukocyte and the EC, along with junctional proteins between ECs, which redistribute during transmigration (Carman *et al.*, 2007; Carman and Springer, 2008; Mamdouh *et al.*, 2009).

Rho GTPases are critical components of the EC signaling pathways that control cell junctions (Aghajanian *et al.*, 2008; Wittchen, 2009; Daniel and van Buul, 2013). Signals are generated by soluble inflammatory mediators, such as tumor necrosis factor α (TNFα), and by cell-surface adhesion molecules, such as intercellular adhesion molecule 1 (ICAM-1; Stolpen *et al.*, 1986; Clark *et al.*, 2007; Muller, 2009). These primary signals activate Rac1 and RhoA in the EC, leading to controlled perturbations in the monolayer (Wojciak-Stothard *et al.*, 1998; Wojciak-Stothard and Ridley, 2002; van Wetering *et al.*, 2002; Nwariaku *et al.*, 2003) and actions that facilitate leukocyte transmigration (van Wetering *et al.*, 2003; Wittchen, 2009; Daniel and van Buul, 2013). Rac1 and RhoG promote formation of the actin-based, cup-shaped structure that docks the transmigrating leukocyte (van Buul *et al.*, 2007; van Rijssel *et al.*, 2012) and also coordinates downstream signaling. Cortactin in endothelial cells has been shown to play a critical role in many steps during transmigration (Tilghman and Hoover, 2002; Yang *et al.*, 2006a,b). However, nothing is known about other Arp2/3 complex regulators downstream of Rac, and little is known about the how Arp2/3 complex contributes to the various steps during transmigration.

Martinelli *et al.* (2013) described roles for Rac1 and Arp2/3 complex in pore closure after transmigration of T-lymphocytes. They found that ECs use directional lamellipodial protrusions to close lymphocyte transmigration pores. They concluded that Rac1 activation promoted the formation of these lamellipodia, based on effects of the Rac1 inhibitor NSC23766 and by overexpression of dominant-negative Rac1. They also used an inhibitor of Arp2/3 complex, CK-666, to demonstrate that these lamellipodia depended on the activity of Arp2/3 complex.

Rac1 has several downstream effectors other than Arp2/3 complex, and a number of proteins are able to recruit and activate Arp2/3 complex; therefore we chose to focus on the role of the specific effector WAVE2, and we used molecular genetic approaches specific for WAVE2. Rac1 recruits and activates WAVE2 at locations where formation of Arp2/3-mediated dendritic actin networks are required. WAVE2 is one subunit of a pentameric protein complex that promotes actin nucleation by Arp2/3 complex (Ibarra *et al.*, 2005; Campellone and Welch, 2010; Derivery and Gautreau, 2010). In ECs, WAVE2 is known to be important for lamellipodia formation (Yan *et al.*, 2003; Yamazaki *et al.*, 2005, 2007; Bryce *et al.*, 2013) and for directed cell migration (Yamazaki *et al.*, 2003).

In this study, we asked how Arp2/3 complex–dependent F-actin networks contribute to transmigration at each step of the process. We used perturbation of WAVE2 to provide insight into the role of Arp2/3 complex during transmigration. We analyzed the dynamics of living ECs and lymphocytes in a primary-cell culture system using time-lapse movies, fluorescent fusion proteins, and RNA interference–mediated gene targeting. We found that actin assembly downstream of WAVE2 in ECs is necessary to engage transmigrating lymphocytes, promote the transcellular route of migration, and close junctional pores after the lymphocyte moves away. We also found that WAVE2 is necessary for endothelial monolayer integrity, which is a critical determinant of overall transendothelial migration, especially the paracellular route.

RESULTS

To begin TEM, lymphocytes adhere to the endothelial monolayer and walk along its apical surface (Supplemental Movie S1 and Figure 1A). Docking structures form on the EC and bind the lymphocyte, after which the lymphocyte passes through the endothelium via the paracellular or transcellular route. Supplemental Movie S1 and Figure 1A show an example of the latter.

Docking structure formation: roles of WAVE2 and Arp2/3

The docking structure is an actin-rich membrane protrusion, which forms on the surface of the EC as the leukocyte comes in contact (Barreiro *et al.*, 2002; Carman *et al.*, 2003; Carman and Springer, 2004). The docking structure promotes the physical interaction between the two cells, and it serves as a hub for generation and regulation of signals that drive the subsequent processes of transmigration in both ECs and leukocytes.

We hypothesized that WAVE2 might function in docking structure formation to recruit and activate Arp2/3 complex and induce the actin assembly that drives protrusions. To test this hypothesis, we induced docking structures to form on ECs in monolayers using polystyrene beads coated with anti–ICAM-1 instead of lymphocytes. The anti–ICAM-1 on the bead clusters the integrin receptor ICAM-1 on the surface of the EC (Tilghman and Hoover, 2002; van Buul *et al.*, 2007; van Rijssel *et al.*, 2012), mimicking the action of LFA-1 on the lymphocyte (van Buul *et al.*, 2007). The docking structures induced by anti–ICAM-1–coated beads resemble those induced by lymphocytes in terms of morphology and molecular composition. The use of beads allows one to focus exclusively on endogenous components of the EC, avoiding signals from lymphocytes.

Using immunofluorescence, we observed endogenous Arp2/3 complex, WAVE2, and F-actin on EC docking structures created by anti–ICAM-1 beads (Figure 1B). ICAM-1 clustered around most beads, and nearly every ICAM-1–positive bead recruited WAVE2, Arp2/3 complex, and F-actin, which appeared as rings around the beads. If beads did not cluster ICAM-1, they did not recruit WAVE2, Arp2/3 complex, or F-actin. We conclude that ICAM-1 clustering is necessary and sufficient for recruitment of WAVE2, Arp2/3, complex and F-actin and that the process of docking structure assembly is robust.

We assessed the role of WAVE2 in docking structure formation by depleting WAVE2 with small interfering (siRNA). We chose an oligonucleotide that decreased WAVE2 protein levels (see *Materials and Methods* and Supplemental Figure S1A), and we documented specificity by rescue with expression of siRNA-resistant WAVE2. Anti–ICAM-1 beads adhered to WAVE2-depleted cells to a similar extent as observed for control cells; however, the recruitment of Arp2/3 complex and F-actin was decreased (Figure 1C). For Arp2/3 complex, 15.5 ± 5.7% (median ± SE of proportion [SEp], $N = 40$ fields of view [fov]) of beads stained for Arp2/3 complex in WAVE2-depleted monolayers, compared with 34.6 ± 7.5% ($N = 40$ fov) in control monolayers. For F-actin, 9.0 ± 5.2% (median ± SEp, $N = 30$ fov) of beads stained for F-actin in WAVE2-depleted monolayers, compared with 33.7 ± 8.6% ($N = 30$ fov) in controls (Figure 1D).

The defect in recruitment of F-actin was more prominent than the defect in recruiting Arp2/3 complex. In control cells, only 3.5 ± 0.6% (mean ± SEp, $N = 857$ rings) of bead-associated rings that were positive for Arp2/3 complex did not stain for F-actin. In contrast, in WAVE2-depleted cells, 33.4 ± 1.9% ($N = 619$ rings) of Arp2/3-positive rings did not stain for F-actin. We conclude that WAVE2 both recruits and activates Arp2/3 complex in the EC in order to induce actin assembly and generate docking structures.

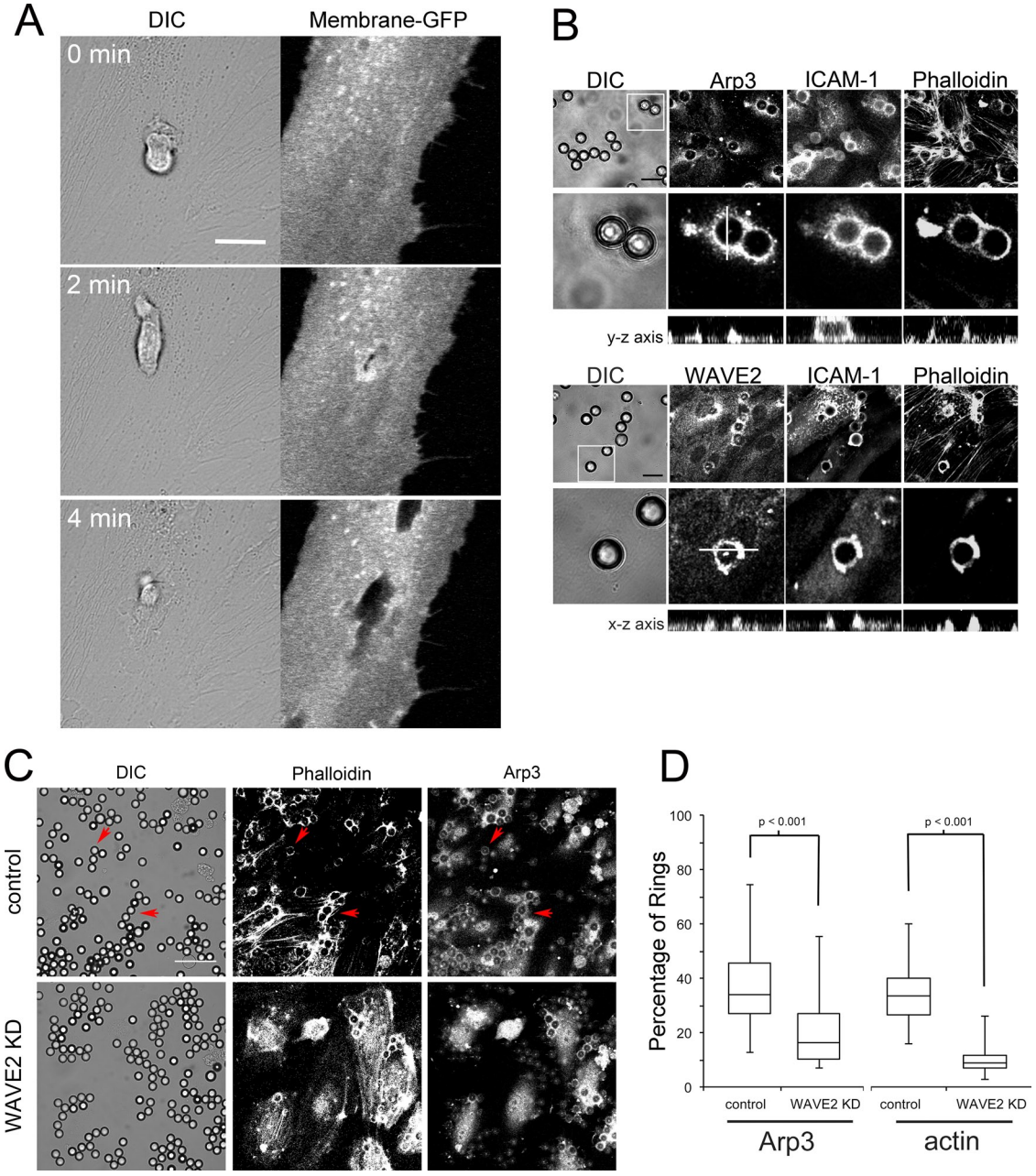

FIGURE 1: WAVE2 and Arp2/3 complex are important for docking structure formation. (A) Frames from Supplemental Movie S1 show a lymphocyte undergoing transcellular transmigration through an EC expressing membrane-tagged GFP. Scale bar, 10 μm. (B) WAVE2, Arp2/3 complex, and F-actin colocalize with rings of ICAM-1 that form around anti–ICAM-1–coated beads in contact with ECs after 30 min of incubation. The *yz*- and *xz*-projections from three-dimensional (3D) data sets reveal membrane protrusions extending upward to cup the beads. Scale bar, 20 μm. (C) WAVE2 depletion decreases the number of bead-associated rings stained for F-actin and Arp2/3 complex. Red arrows indicate rings of F-actin and Arp2/3 complex around anti-ICAM-1 beads. Scale bar, 50 μm. (D) WAVE2 depletion decreases the number of beads with associated rings of F-actin and Arp2/3 complex. Beads and positive-stained rings were counted in 10 fov for three separate experiments ($N = 30$). Box-and-whisker plots show median, interquartile range, and extremes.

Recruitment of WAVE2 during transmigration of lymphocytes

After docking structures form, lymphocytes traverse the monolayer by migrating between cells (paracellular route) or through individual ECs (transcellular route). For both routes, we observed recruitment of WAVE2–green fluorescent protein (GFP) in the EC to the site of transmigration by peripheral blood lymphocytes (PBLs) at distinct times during the process.

For the paracellular route, PBLs migrated over the course of 2–5 min through a pore that formed between two ECs. The pore often remained open for several minutes after the PBL moved away from the transmigration site (Figure 2A; asterisk indicates a persisting pore). WAVE2-GFP did not accumulate at the transmigration site either before or during transmigration (Figure 2A and Supplemental Movie S2). When the pores closed, if the pore size was large, ECs produced waves of membrane protrusion as they

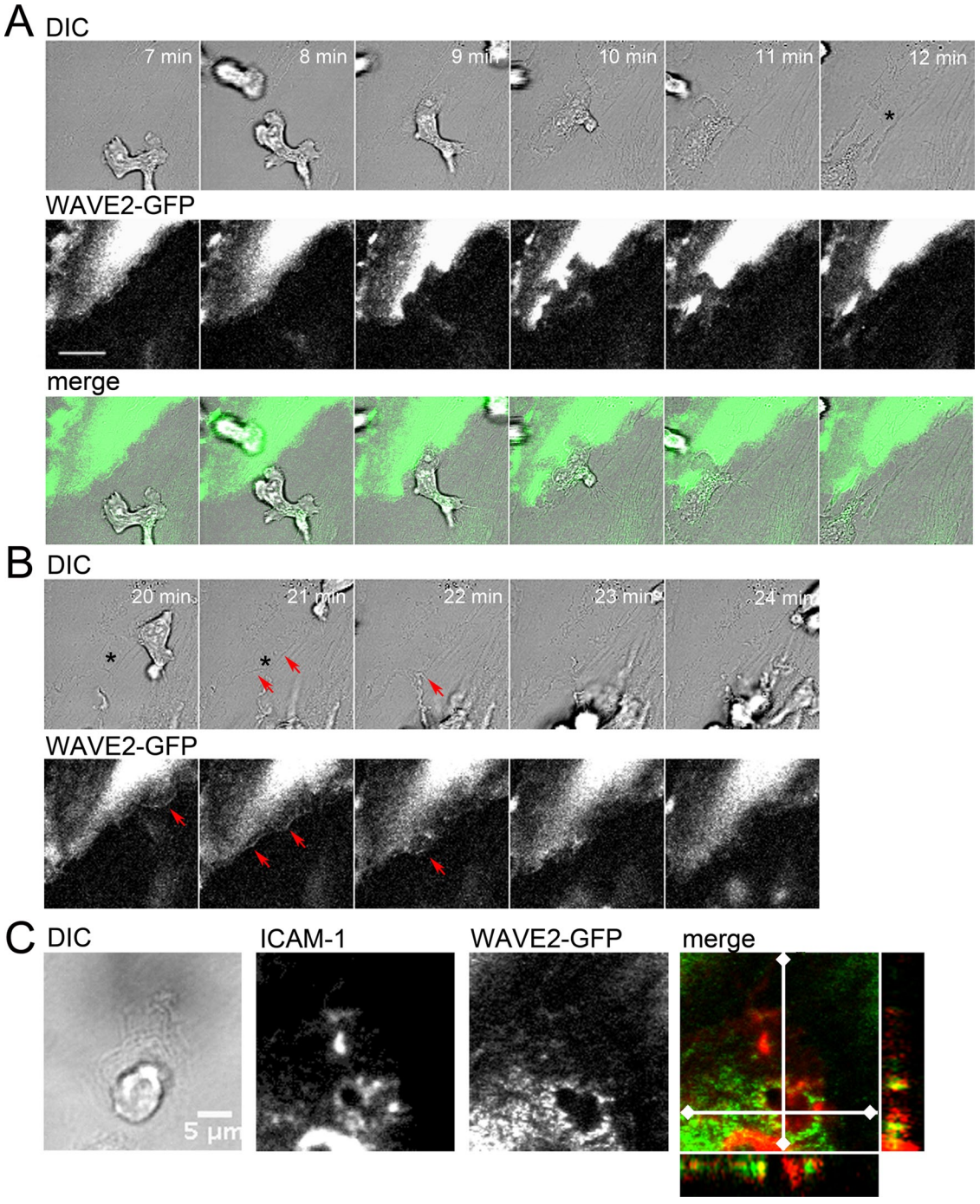

FIGURE 2: WAVE2 localization to membrane protrusions that close gaps and form at sites of transcellular pores. (A) WAVE2 is not recruited to paracellular pores during PBL transmigration. Frames from Supplemental Movie S2. Asterisk indicates a gap between ECs that persists after transmigration. Scale bar, 3 µm. (B) WAVE2 localizes to endothelial monolayer gaps that close after lymphocyte transmigration. Frames from Supplemental Movie S3. Asterisks indicate the gap, which closes after a wave of membrane protrusion. Red arrows indicate membrane waves, where WAVE2 has accumulated. Scale bar, 3 µm. (C) WAVE2 localizes to docking structures at sites of transcellular migration. ECs expressing WAVE2-GFP and immunolabeled for ICAM-1. Transmigrating lymphocyte is shown in the DIC image. The *yz*- and *xz*-projections from a 3D data set reveal WAVE2 in membrane protrusions that cup the PBL.

closed the gap. WAVE2-GFP localized at the front of these protrusions, which traveled laterally along the edge of the EC (Figure 2B and Supplemental Movie S3). This dynamic behavior is consistent with the idea that WAVE2 activates Arp2/3 complex and promotes actin assembly to drive the formation and extension of membrane protrusions. Small pores sometimes closed rapidly, without membrane protrusions, and WAVE2-GFP did not accumulate.

The transcellular route occurred less frequently in cells expressing WAVE2-GFP, and the degree of inhibition appeared to be proportional to the expression level, so we suspect that the expression had a dominant negative effect. This effect limited the number of

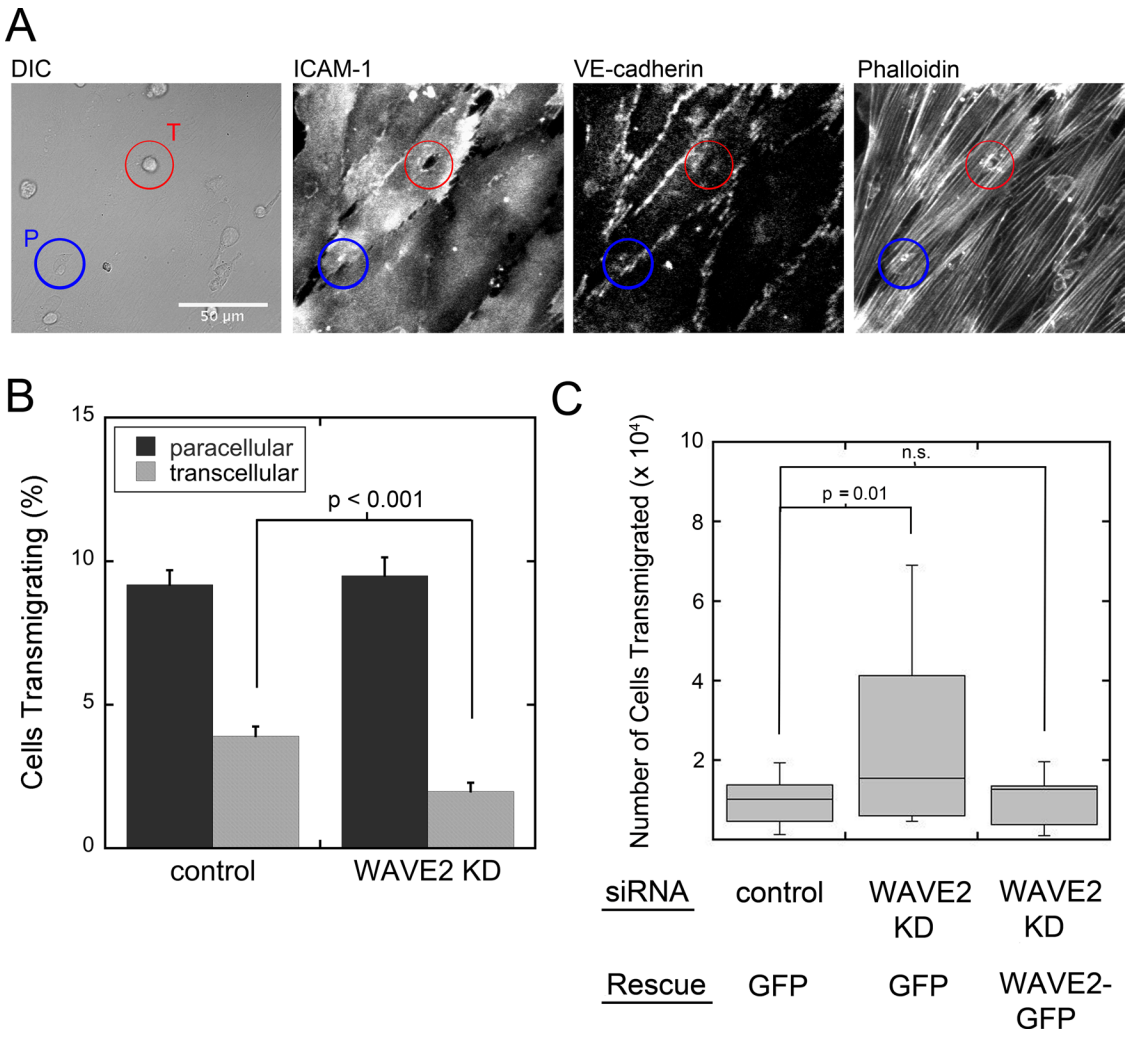

FIGURE 3: WAVE2 is important for the transcellular route of lymphocyte transmigration and bulk migration of lymphocytes across endothelial monolayers. (A) Representative images illustrating the transcellular route (red) and paracellular route (blue). An endothelial monolayer with transmigrating lymphocytes was stained for ICAM-1, VE-cadherin, and F-actin. (B) Quantification of the routes of transmigration by lymphocytes (PBLs). The percentage of total PBLs that transmigrate by the paracellular or the transcellular route was calculated. Data from experiments on three separate days are combined and plotted as the mean and SE of proportion (control EC monolayers, $N = 3330$ PBLs; WAVE2-knockdown EC monolayers, $N = 2167$ PBLs). (C) WAVE2-knockdown endothelial monolayers show increased transendothelial migration by lymphocytes in Transwell assays. Box-and-whisker plots show the median, the interquartile range, and the extremes of the number of transmigrated cells ($N = 14$).

transcellular-route events available for movie analysis. As an alternative approach, we used fixed and stained preparations, which allowed us to examine many large fields of view in order to visualize a sufficient number of events. Fluorescence imaging of anti–ICAM-1 and WAVE2-GFP revealed that WAVE2 was recruited to sites of transcellular TEM in ECs (Figure 2C). Accumulation of WAVE2 was greatest at early stages of transcellular TEM, such as during docking structure formation, with lesser amounts of WAVE2 observed at later stages, when PBL migration through the pore was near completion. In these fixed preparations, identification of pores in the process of closing is problematic because PBLs often migrate away from the pore before closure. Therefore we were not able to assess WAVE2 recruitment to sites of transcellular pore closure.

Relative importance of WAVE2 in transcellular and paracellular routes

To quantitate the effect on WAVE2 depletion on TEM, we first used a conventional Transwell assay with an endothelial monolayer on the filter separating the upper and lower chambers. We measured the number of PBLs that migrated from the upper to the lower chamber. WAVE2 depletion increased the number of PBLs that transmigrated (Figure 3C). However, the level of variation between experiments was large with this assay; in some cases, the number of transmigrating PBLs did not change or decreased. We speculate that this high level of variance in the assay resulted from variations in the morphology of the EC monolayer caused by WAVE2 depletion, which was associated with gaps between ECs of variable number and size. The effect of WAVE2 depletion on EC monolayer morphology is discussed in more detail later. Expression of siRNA-resistant WAVE2 restored PBL transmigration to levels similar to that in control endothelial monolayers (Figure 3C).

To address the role of WAVE2 in TEM with a quantitative assay that would not depend so highly on gaps in the monolayer, we used a different approach. We fixed TEM preparations and stained them with anti–VE-cadherin to reveal EC junctions, anti–ICAM-1 to reveal transendothelial pores, and fluorescent phalloidin to visualize

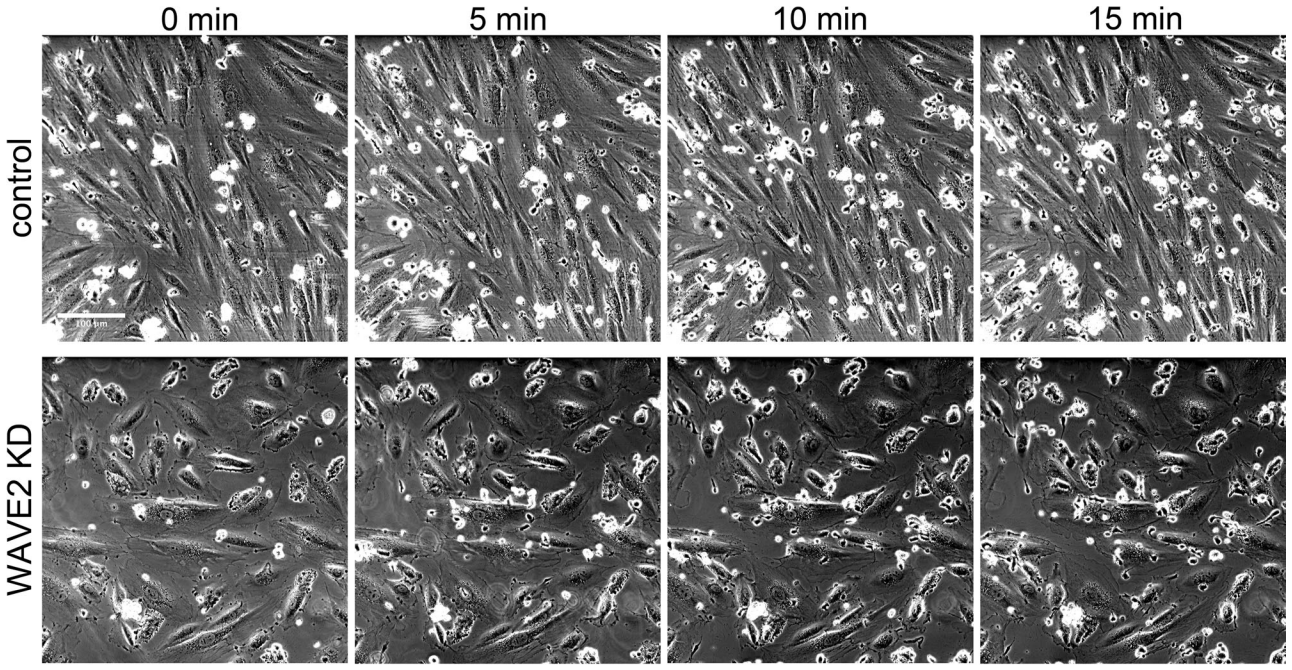

FIGURE 4: WAVE2 is necessary for limiting gaps and promoting spread-cell morphology in endothelial-cell monolayers. Images are frames from movies, with control from Supplemental Movie S5 and WAVE2 KD (knockdown) from Supplemental Movie S4. Scale bar, 100 μm.

migrating PBLs (Figure 3A). This approach allows one to identify paracellular-route and transcellular-route sites of TEM with certainty. Paracellular-route sites were defined by PBLs at cell junctions, intercalated between two adjacent ECs, which were not otherwise separated by a gap. Transcellular-route sites were defined by PBLs at pores in the central region of an EC that was fully spread and in contact with its neighbors in the monolayer.

Using this approach, we found that depletion of WAVE2 from EC monolayers decreased the frequency of transcellular TEM events to 51% of the value seen with control EC monolayers; the difference was highly significant ($p < 0.001$; Figure 3B). In contrast, the frequency of paracellular TEM events did not change (Figure 3B). Thus WAVE2 is more important for the transcellular route than the paracellular route. Using these fixed and stained preparations, we measured the dimensions of the pores for transcellular-route events in the *x-y* plane and found no difference between control and WAVE2-depleted cells. The area of the pores was 37.3 ± 7.7 μm^2 (mean ± SE, $N = 12$) for control cells and 37.6 ± 6.9 μm^2 ($N = 8$) for WAVE2-depleted cells. We conclude that WAVE2 is important for transcellular-route events to occur, but that when the events do occur, the pores have a normal size, which is presumably determined by the size of the migrating cells. For the paracellular route, measuring pore dimensions was confounded by the many gaps between ECs in WAVE2-depleted monolayers. Finally, we attempted to examine the dynamics of transcellular pore formation and closure using movies of living cell movies, but the number of transcellular-route events in WAVE2-depleted monolayers was too small to allow meaningful conclusions.

WAVE2 is important for integrity of the endothelial monolayer

As noted earlier, we observed many intercellular gaps in WAVE2-depleted monolayers (Supplemental Movie S4 and Figure 4). Cells within WAVE2-depleted endothelial monolayers also displayed a wide range of individual morphologies. Many were rounded up and no longer in contact with their neighbors. In movies, these cells were often blebbing very actively, and they made frequent attempts to spread back down onto the surface (Supplemental Movie S4). Scoring cells on their morphology, we found that WAVE2-depleted monolayers had 34.7 ± 23.8% (mean ± SEp, 814 cells, four movies) rounded-up or blebbing cells, whereas control monolayers had only 0.20% ± 1.99% (968 cells, five movies). This difference was statistically significant, with $p < 0.01$. Expression of siRNA-resistant WAVE2-GFP rescued this phenotype, leading to nearly complete absence of cells with the rounded-up and blebbing morphology (1.8 ± 0.8%, 402 cells, three movies; Supplemental Movie S6). The *p* value for control versus WAVE2 rescue was 0.13.

Movie analysis also revealed that addition of PBLs to control EC monolayers often caused effects at contacts between EC neighbors, even when PBLs were located at a distance. These effects consisted of dynamic ruffling at cell–cell junctions, along with the occasional formation of small gaps as cells pulled away from one another while ruffling (Supplemental Movie S5 and Figure 4). When such a gap appeared, lamellipodial protrusions formed quickly and closed the gap. In WAVE2-depleted monolayers, the number of gaps was high, as noted earlier, and there were fewer lamellipodial protrusions that closed gaps between cells than with control monolayers.

On the basis of these observations of EC monolayers, we hypothesized that WAVE2 depletion might cause defects in the overall integrity of the endothelial barrier measured by conventional physiological assays. To test this hypothesis, we first measured electrical resistance across the monolayer (transendothelial resistance [TER]; Figure 5A). WAVE2 depletion caused TER to decrease to levels similar to those caused by chelation of Ca^{2+}, which completely disrupts cadherin-based cell–cell junctions. Depolymerizing actin with latrunculin A (LatA) also decreased TER by a large amount (Figure 5A) and created large gaps between ECs (Supplemental Figure S1B), consistent with previous findings (Prasain and Stevens, 2009). Second, we

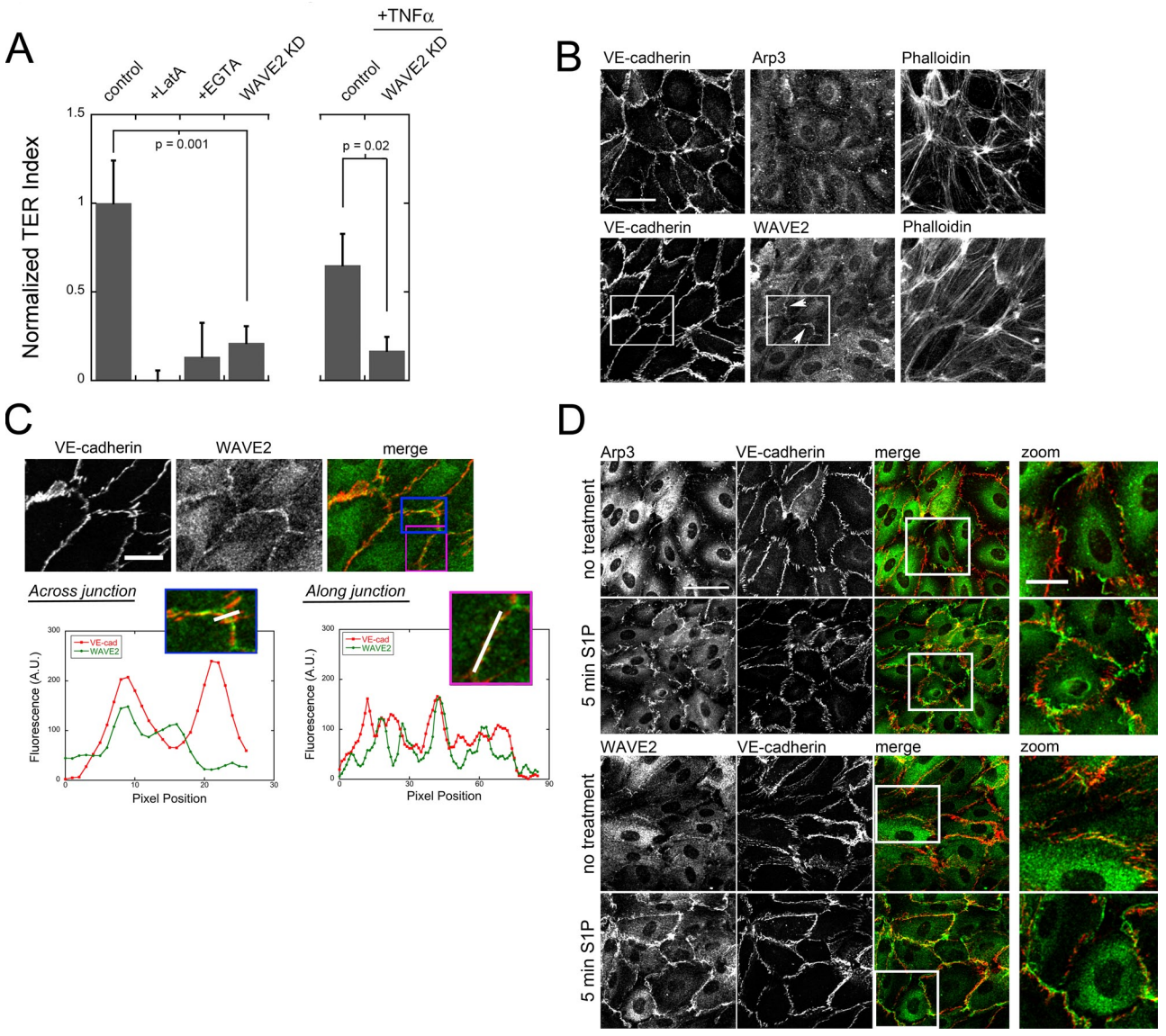

FIGURE 5: WAVE2 maintains endothelial monolayer integrity by promoting Arp2/3-based lamellipodial protrusions. (A) Electrical resistance across monolayers, plotted as a normalized index for TER (see *Materials and Methods*). Data are derived from experiments on three or more days, with three or more repetitions on each day. Plotted values are the mean of all the data points, and error bars are SD ($N \geq 9$). (B) Localization of WAVE2 and Arp2/3 complex adjacent to cell–cell junctions, based on immunofluorescence and fluorescent phalloidin staining of endothelial monolayers. Arrows indicate localization close to but not coincident with cell junctions. Scale bar, 50 μm. (C) Magnified views of boxed regions in B. Line scans across cell–cell junctions (blue box) or along junctions (magenta box). Scale bar, 20 μm. (D) Localization of Arp2/3 complex and WAVE2 at cell–cell junctions formed in response to S1P. Merge, green is anti-Arp3 or anti-WAVE2; red is VE-cadherin. Top, control; bottom, with S1P added. Scale bar, 50 μm; inset, 20 μm.

measured the permeability of the monolayer to fluorescent dextran, as an indicator of barrier integrity. Again, EC monolayers depleted of WAVE2 showed increased permeability compared with control (Supplemental Figure S1C).

In our experiments, the endothelial monolayers were generally treated with the proinflammatory molecule TNFα in order to mimic inflammatory conditions and promote interaction of ECs with PBLs. Inflammation increases vascular permeability, so we asked whether TNFα alone would affect barrier integrity in these assays. In control cells, TER decreased with TNFα treatment (Figure 5A), as expected (Blum *et al.*, 1997; Nwariaku *et al.*, 2003; Clark *et al.*, 2007). Quantitatively, the effect of TNFα on control monolayers was modest compared with the large effect of LatA or ethylene glycol tetraacetic acid (EGTA). The effect of WAVE2 depletion was also relatively large, and the addition of TNFα had little to no further effect. Similar results were seen using the fluorescent dextran permeability assay (Supplemental Figure S1C). Together the results indicate that WAVE2 depletion results in an essentially complete loss of endothelial monolayer integrity, in excess of the effect caused by TNFα.

How might WAVE2 contribute to endothelial monolayer integrity? We reasoned that WAVE2 might localize to cell edges and activate Arp2/3 complex, causing protrusions that initiate contacts between cells as a prelude to cell–cell junction formation. Lamellipodial protrusions have been implicated in the formation of junctions between epithelial cells (Adams *et al.*, 1996), and lamellipodia

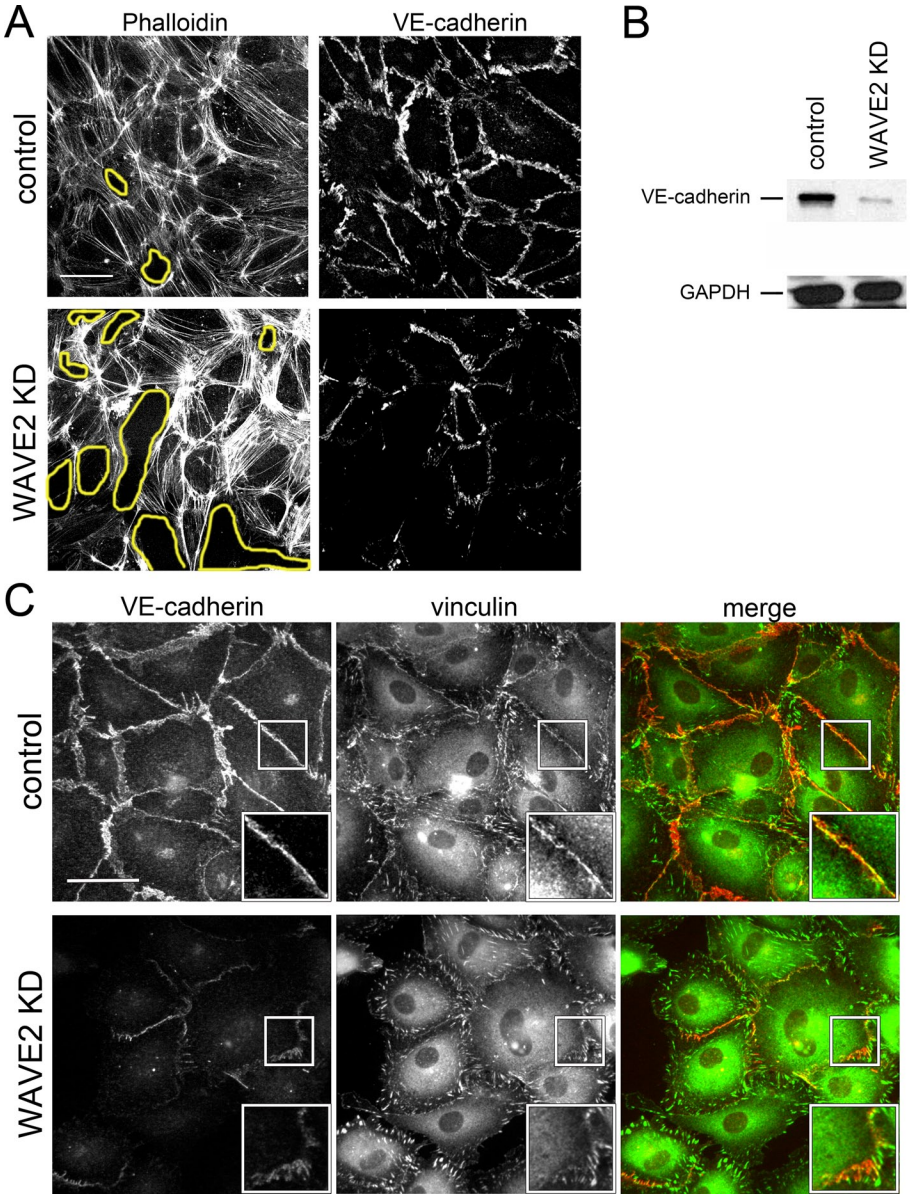

FIGURE 6: WAVE2 promotes VE-cadherin expression and maturation of cell–cell junctions. (A) WAVE2-knockdown monolayers have large gaps between cells, outlined in yellow, and the intensity of VE-cadherin staining is substantially decreased. Scale bar, 50 μm. (B) Decreased total VE-cadherin in WAVE2-knockdown monolayers, by immunoblot. (C) Depletion of WAVE2 leads to a change from mature junctions, collinear with the cell edge, to immature junctions perpendicular to the cell edge, based on staining for VE-cadherin and vinculin. Scale bar, 50 μm.

have been observed during initial formation of cell–cell contacts between ECs (Hoelzle and Svitkina, 2012). Information about the molecular components that establish junctions or maintain junctional integrity of ECs is lacking, but the Arp2/3 complex has been implicated in maintaining intact endothelial monolayers (Taha *et al.*, 2014).

First, we found that WAVE2 was localized near or next to cell junctions between ECs but not coincident with junctions in fixed and stained preparations (Figure 5, B and C). Line scans of fluorescence intensity across or along junctions demonstrated that VE-cadherin and WAVE2 were frequently adjacent to, but infrequently coincident with, each other (Figure 5C). The localization of Arp2/3 complex around cell junctions was similar to that of WAVE2 (Figure 5B), consistent with a recent report (Taha *et al.*, 2014).

Second, movies revealed that dynamic lamellar and lamellipodial protrusions formed along the cell periphery and in the vicinity of cell–cell junctions (Supplemental Movie S7). These protrusions contained WAVE2 at their leading edge (Supplemental Movie S8), which supports the idea that WAVE2 and Arp2/3 complex drive actin assembly in order to promote formation of cell junctions and repair gaps between cells. Consistent with this notion, Taha *et al.* (2014) used chemical inhibitors of Arp2/3 complex to demonstrate that Arp2/3-based lamellipodial protrusions exist and are important to maintain the endothelial monolayer.

To test this hypothesis further, we increased the number of membrane protrusions by treating endothelial monolayers with sphingosine-1-phosphate (S1P; Supplemental Figure S2). Ruffling lamellipodia and lamellar protrusions induced by S1P contained WAVE2 and Arp2/3 complex (Figure 5D). VE-cadherin did not colocalize with Arp2/3 or WAVE2, indicating that WAVE2 and Arp2/3 complex promote lamellipodial protrusions before the recruitment of VE-cadherin to nascent cell–cell junctions.

Molecular basis for loss of monolayer integrity on WAVE2 depletion

To investigate the molecular basis for the loss of monolayer integrity upon depletion of WAVE2, we examined the molecular composition of cell contacts and cell–cell junctions using immunofluorescence. In control monolayers, VE-cadherin was predominantly organized in a pattern typical for mature junctions—continuous linear structures coinciding with cell–cell contacts (Figure 6A). In contrast, WAVE-depleted monolayers showed very few VE-cadherin–positive cell junctions (Figure 6A). The number of gaps in the junctions increased from 3.0 ± 1.0/fov (mean ± SD, $N = 6$ fov) in control monolayers to 11.2 ± 2.3/fov in WAVE2-knockdown monolayers. This difference was statistically significant, with $p < 0.001$.

We quantitated the level of VE-cadherin at cell junctions in the immunofluorescence images. In control cells, the level of anti–VE-cadherin fluorescence intensity was 37.9 ± 2.6 arbitrary units (A.U.) per junction (median ± SE, $N = 126$ junctions from 6 fov). In WAVE2-depleted cells, for the cell junctions that were present, the anti–VE-cadherin fluorescence intensity was 12.6 ± 3.7 A.U. (median ± SE, $N = 99$ junctions from 6 fov). This difference was also highly statistically significant, $p < 0.001$. In addition, immunoblot analysis revealed that the total level of VE-cadherin expression was decreased in WAVE2-depleted ECs (25.6 ± 0.2%, mean ± SEp, $N = 4$, $p = 0.01$) compared with control cells (Figure 6B).

In contrast, a similar analysis of the tight junction component ZO-1 showed little to no change upon depletion of WAVE2. Qualitatively, by immunofluorescence, ZO-1 was readily observed at

persisting junctions in WAVE2-depleted cells, with a pattern and intensity similar to those of control cells (Supplemental Figure S3A). Immunoblots revealed only a small decrease of ZO-1 protein expression; the level in WAVE2-depleted cells was 88% (average of two experiments) of the level in control cells (Supplemental Figure S3B).

The junctions that were present in WAVE2-depleted monolayers appeared to be immature, based on morphology and vinculin content (Figure 6C). Mature cell–cell junctions in control EC monolayers, defined by linear anti–VE-cadherin staining coincident with cell–cell contacts, displayed a low level of anti-vinculin staining (Figure 6C, top). In control monolayers, vinculin was also present at focal contacts, which are cell–substrate junctions devoid of VE-cadherin (Figure 6, C and inset). In WAVE2-depleted monolayers, the VE-cadherin at persisting junctions was organized as short, linear structures oriented perpendicular to the cell edge (Figure 6, C and inset), characteristic of immature cell–cell junctions (Heyraud *et al.*, 2008; Huveneers *et al.*, 2012). In a quantitative analysis, the number of mature junctions decreased from 8.7 ± 2.9/fov in control monolayers to 2.7 ± 0.8/fov in WAVE2-depleted monolayers (mean ± SD, $N = 6$ fov; $p < 0.001$).

Functional ability of WAVE2-depleted ECs to form cell–cell junctions

To investigate further the role of WAVE2 in cell junction formation, we challenged EC monolayers to assemble junctions by Ca^{2+} depletion and addition (Figure 7, Supplemental Figure S4, and Table 1). VE-cadherin–based junctions are lost when Ca^{2+} is removed, and they assemble when Ca2+ is added back. We found that depletion of WAVE2 impaired the efficiency of ECs to form cell junctions in this assay (Figure 7, Supplemental Figure S4, and Table 1). At all time points during reassembly, the number of junctions in WAVE2-depleted monolayers was lower than in control monolayers (Figure 7, Supplemental Figure S4, and Table 1). When junctions re-formed in the WAVE2-depleted monolayers, the fluorescence intensity of the tight-junction protein ZO-1 was similar to that in control monolayers (Figure 7 and Table 1).

Using a complementary quantitative approach, we measured TER on control and WAVE2-depleted monolayers after calcium depletion and repletion (Figure 7B). WAVE2-depleted monolayers had a lower initial value for TER, as reported earlier, and they had lower TER values under all treatment conditions. However, when the TER values were normalized, the rate at which WAVE2-depleted monolayers recovered their junctions was similar to that for control monolayers. This result is consistent with the observation that ZO-1 levels are not altered in WAVE2-depleted junctions.

Taken together, our results show that WAVE2 has an important role in promoting the expression or stability of VE-cadherin and its recruitment to cell junctions. This role is similar to the role proposed for WAVE2 in epithelial cells (Bryce *et al.*, 2013). We conclude that the role of WAVE2 in endothelial monolayer integrity is the formation and maturation of cell–cell junctions.

WAVE2 influences the organization of circumferential actin and stress fibers

In addition to lamellar protrusions, ECs contain two other F-actin-based structures important for monolayer integrity—stress fibers and circumferential actin structures. These structures contain myosin-II, which is contractile, and they are able to create tension. In epithelial cells, WAVE2 has been implicated in regulating assembly of circumferential actin (Verma *et al.*, 2012). In ECs, circumferential actin is less dense and more loosely organized; the formation and function of this structure in ECs have not been studied.

Many WAVE2-depleted cells displayed rounded-up and blebbing morphologies, as noted earlier. These cells did not contain either circumferential F-actin or stress fibers (Supplemental Figure S5A, red stars). Therefore, for this analysis, we focused on cells that were in a monolayer and fully spread. We observed that the fluorescence intensity of myosin-II and F-actin in circumferential F-actin fibers in such cells was increased in WAVE2-depleted endothelial monolayers compared with control-cell monolayers (Figure 8, A and B). This finding suggests that increased tension from circumferential actin causes WAVE2-depleted cells to round up.

If this hypothesis is correct, then one would expect increased tension to result in decreased area in well-spread cells in WAVE2-depleted monolayers. As expected, the area of well-spread cells in WAVE2-knockdown monolayers was smaller (1980.8 ± 92.2 μm^2, mean ± SE, $N = 99$) than that of control cells (2430.2 ± 116.7 μm^2, $N = 71$). The difference was statistically significant, with $p = 0.003$.

However, we found that the total levels of F-actin and myosin-II were not affected by WAVE2 depletion. The total level of myosin-IIA fluorescence staining per cell was similar for WAVE2-knockdown and control monolayers, with intensity values of $6.0 \times 10^6 \pm 3.3 \times 10^6$ A.U. (median ± SD, $N = 99$ cells) and $5.6 \times 10^6 \pm 4.1 \times 10^6$ A.U. ($N = 71$ cells), respectively ($p = 0.9$). The level of F-actin, determined by immunoblots of detergent-resistant cytoskeletons (see *Materials and Methods*), was also similar in WAVE2-knockdown and control cells (Supplemental Figure S5B).

Considering these results together, we suggest that depletion of WAVE2 shifts F-actin and myosin-II into the circumferential F-actin fiber pool, which increases tension. Increased tension, in turn, decreases cell size and increases the likelihood that cell lose contact and round up.

Previous studies of endothelial monolayers found that inflammatory conditions lead to loss of monolayer integrity, in association with decreased circumferential actin and increased stress fibers (Stolpen *et al.*, 1986; Blum *et al.*, 1997; Clark *et al.*, 2007). First, we confirmed these results in our preparations; control-cell monolayers treated with TNFα showed loss of circumferential actin with increased stress fibers (Figure 8C, left, arrows, and right, arrows). Next we observed that depletion of WAVE2 prevented these TNFα-induced changes. Circumferential actin staining was increased, not decreased, and stress fibers did not increase (Figure 8C). Thus the inflammatory effects of TNFα require the presence of WAVE2, presumably due to effects on dynamic actin assembly.

Overall our results show that WAVE2 enhances the assembly and influences the organization of circumferential actin fibers. We also conclude that WAVE2 is important for the reorganization of fibers under inflammatory conditions, most likely by an indirect mechanism.

DISCUSSION

The most important finding of our study is that ECs use WAVE2 to create Arp2/3-based actin filament networks necessary for lymphocyte transmigration. EC WAVE2 appears to activate Arp2/3 complex and thereby promote actin assembly at the docking structures that bind lymphocytes to the EC. We also found a role for WAVE2 and Arp2/3 complex in generating lamellipodial protrusions that contribute to the integrity of EC monolayers by closing gaps caused by inflammatory conditions or transmigrating lymphocytes. Our results provide insight into the tissue-level mechanisms by which the vascular endothelium maintains a dynamic barrier and selectively orchestrates transmigration during inflammation.

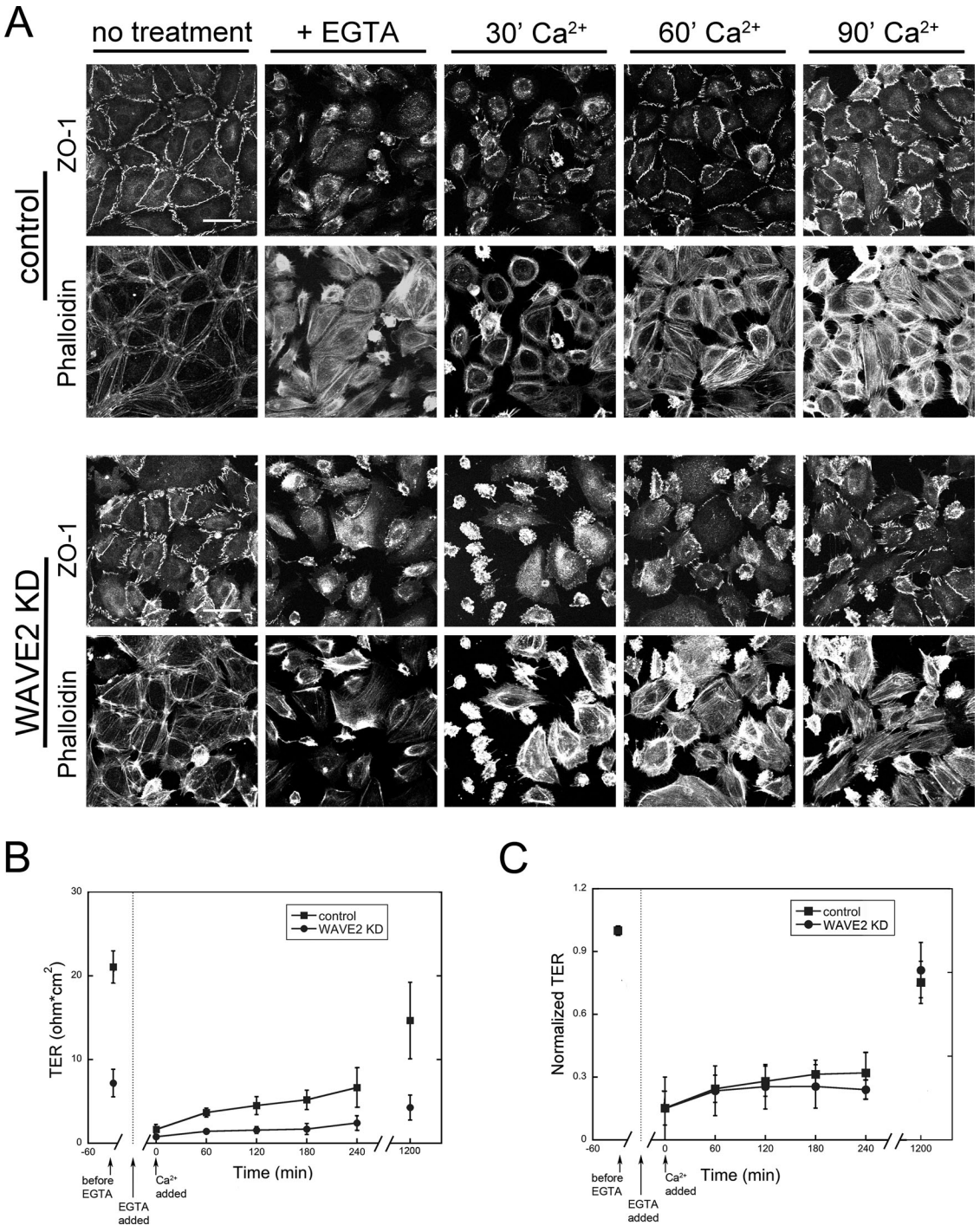

FIGURE 7: WAVE2 is important for junction assembly after calcium depletion and addition. (A) Calcium was removed from the medium with EGTA to disassemble cadherin-based junctions and then replaced to induce reassembly. Images are representative of 5 fov from each of three samples. Scale bar, 50 μm. (B) WAVE2 knockdown causes a defect in junctional assembly after calcium addition, based on TER measurements over time. (C) Time course of junction assembly revealed by the TER data from B normalized for control and WAVE2-depleted monolayers. The time courses are similar, suggesting that junctions recover at a normal rate.

Endothelial WAVE2 controls transmigration of lymphocytes

In an early step in transmigration, docking structures form on the surface of ECs; membrane protrusions formed by dynamic actin assembly reach up and surround the lymphocyte (Barreiro *et al.*, 2002; Carman and Springer, 2004; van Buul *et al.*, 2007). Here we found that WAVE2 and Arp2/3 complex are recruited to these membranes and are necessary to form the protrusions and docking structures.

WAVE2 has a critical role in docking structure formation, which may overlap and synergize with roles of other regulators of Arp2/3 complex. Dendritic actin network assembly is a multistep process, and other proteins likely assist in recruiting and activating Arp2/3

Parameter	Condition	No treatment	EGTA	Ca^{2+} addition		
				30 min	60 min	90 min
Junctions/fov	Control	24.8 ± 1.8	6.4 ± 1.6	12.8 ± 2.7	45.3 ± 3.1	42.9 ± 2.0
	KD	14.7 ± 2.9*	2.8 ± 0.8	3.9 ± 1.3*	14.3 ± 1.7*	20.5 ± 1.3*
ZO-1 intensity (A.U.)	Control	40.5 ± 0.9	21.5 ± 1.4	42.0 ± 2.1	40.7 ± 1.4	73.1 ± 1.7
	KD	55.7 ± 1.5*	28.4 ± 2.5*	30.5 ± 3.5	42.2 ± 2.3	66.0 ± 2.7

Standard error is reported for the number of junctions per field of view (fov) and for the ZO-1 fluorescence intensity level in arbitrary units. KD is WAVE2 knockdown. Asterisk indicates statistical significance for KD compared with control with $p < 0.001$.

TABLE 1: WAVE2 is necessary for formation of new junctions.

complex. We found that WAVE2 depletion caused a larger defect in the recruitment of F-actin than Arp2/3 complex to docking structures. We detected N-WASP and cortactin in docking structures, confirming previous findings for cortactin (Tilghman and Hoover, 2002; Yang *et al.*, 2006a). Thus, whereas other regulators may contribute to recruitment of Arp2/3 complex, WAVE2 appears to be critical for its activation. In other settings, multiple Arp2/3 regulators play complementary and synergistic roles to bind and activate Arp2/3 complex for actin nucleation (Padrick *et al.*, 2011; Ti *et al.*, 2011; Helgeson and Nolen, 2013). Many Arp2/3 regulators possess multiple domains for interactions with other proteins, which may amplify signals and regulate the assembly of the docking structure.

A second step in lymphocyte transmigration is creation of a pore used by the lymphocyte to cross the endothelial monolayer. A pore can be created by weakening a junction between two ECs (the "paracellular" pathway) or by forming a pore through the interior of one EC (the "transcellular" pathway). We discovered that WAVE2 and Arp2/3 complex are critical for the transcellular pathway. As a transcellular pore develops, the EC controls the size of the pore and provides it with structural stability to preserve cell viability and integrity. We envision that Arp2/3-based filament networks surround the transcellular pore and maintain its size and stability while the lymphocyte is transmigrating. In addition, many membrane-remodeling events occur during transcellular pore formation, and Arp2/3 complex and its activators may be important for those events.

A third step in transmigration is closure of the pore, returning the endothelial monolayer to its original state. We found that, after the lymphocyte transmigrates, lamellipodial protrusions form and fill the pores, allowing ECs to recreate contacts and cadherin-based cell junctions with their neighbors. Actin assembly induced by WAVE2 and Arp2/3 complex drives these lamellipodial protrusions.

How cells and layers of cells close gaps, including ones created by artificially induced wounds, has been studied in a variety of cell and tissue systems. In some cases, closure of the wound involves lamellipodial or filopodial protrusions that extend from cells on the edge of the wound to create new cell–cell contacts (Bement *et al.*, 1993; Jacinto *et al.*, 2001; Mattila and Lappalainen, 2008). In epithelial cell layers and in single egg cells, wounds are often closed by a contractile purse string of F-actin and myosin-II (Martin and Lewis, 1992; Bement *et al.*, 1993, 1999; Sonnemann and Bement, 2011). Here, in ECs, we found that lamellipodial wave-like protrusions of the plasma membrane closed the gaps between cells, consistent with results for closing wounds in other endothelial systems (Martinelli *et al.*, 2013; Taha *et al.*, 2014). Martinelli *et al.* (2013) observed that EC lamellipodia closing transcellular wounds were located in a ventral position. We did not observe ventral lamellipodia in our experiments; however, one can imagine that WAVE2 might also promote the formation and movement of those structures.

WAVE2 promotes and maintains EC junctions by modulating actomyosin organization

We also found that WAVE2 was important for the architecture of actin–myosin structures in ECs, including circumferential F-actin and stress fibers. Resting ECs in monolayers have a loose circumferential band of F-actin and myosin-II near the cell edge, which presumably helps maintain cell–cell junctions and monolayer integrity. In epithelial cells, cell–cell junctions are associated with a denser band of dynamic actin filaments, along with a cortical Arp2/3-based filament network (Ivanov and Naydenov, 2013).

Epithelial cells do not have lamellipodia at mature junctions, in contrast to our findings here with ECs. In epithelial cells, WAVE2 localizes to mature cell junctions, where it regulates actin assembly (Yamazaki *et al.*, 2007; Verma *et al.*, 2012). In our studies here of ECs, WAVE2 and Arp2/3 did not localize to stable cell–cell junctions. Whereas WAVE2 and Arp2/3 complex did localize to the cell periphery and to the locations of cell–cell contacts, their localization and activity were restricted to junctions that were actively assembling, with lamellipodial membrane protrusions.

Tension is an important parameter that determines the strength of the endothelial barrier, one that is highly regulated under resting and inflammatory conditions. For epithelial cells, WAVE2 regulates cell tension in monolayers by affecting the level of contractile myosin-II, the amount of F-actin, and the organization of cortical actin and actin fibers at cell junctions (Verma *et al.*, 2012). Our results here with EC monolayers also suggest that WAVE2 contributes to cell tension by influencing actomyosin organization under both basal and inflammatory conditions. The mechanism for how WAVE2 and Arp2/3-based networks contribute to actin fiber organization remains unclear; we speculate that branched filaments from Arp2/3-based networks incorporate into circumferential filament bundles or stress fibers.

MATERIALS AND METHODS

Cells

Human dermal microvascular ECs from neonates were purchased from Lonza (Basel, Switzerland), maintained in EGM-2MV media (Lonza), and used between passages 2 and 12. PBLs were collected from healthy blood donors (Leukopak; Hemerica, West Warwick, RI) and treated as previously described (Carman and Springer, 2004; Cernuda-Morollon *et al.*, 2010). PBLs were maintained in culture in RPMI with 10% fetal bovine serum (FBS) and interleukin-2 (10 U/ml) for 5–10 d before use in experiments.

Reagents and antibodies

Treatment of cells with TNFα (Life Technologies, Frederick, MD) consisted of overnight incubation at 20 ng/ml. S1P (Sigma-Aldrich, St. Louis, MO) treatment was at 0.5 µM for 5 min. Anti–ICAM-1 antibodies included mouse BBIG-I1 from R&D Systems (Minneapolis, MN) and rabbit H-108 from Santa Cruz Biotechnology (Dallas, TX).

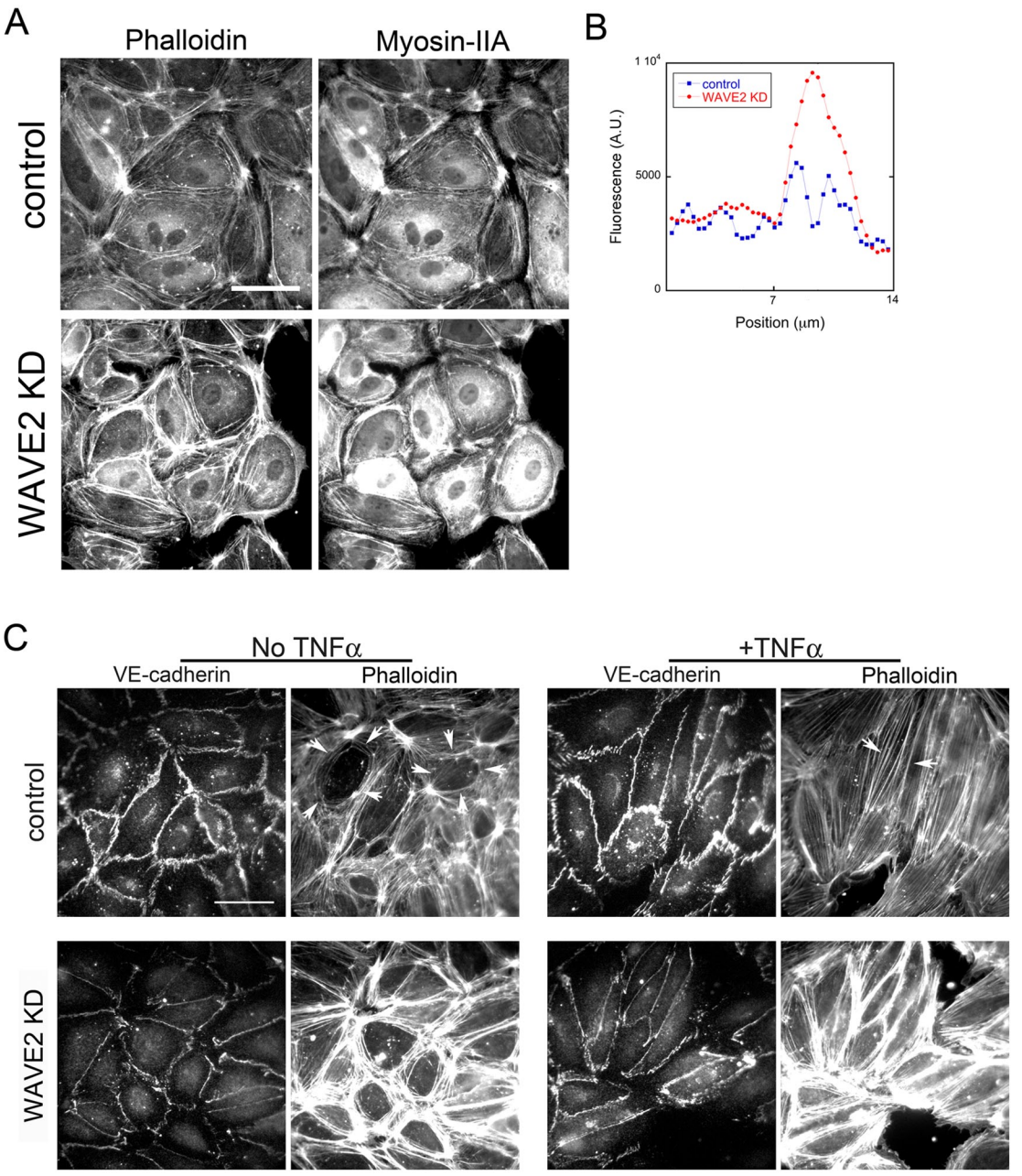

FIGURE 8: WAVE2 controls the organization of actin-myosin fibers in ECs. Areas with well-spread cells were selected to reveal circumferential actin–myosin rings and stress fibers. (A) Control and WAVE2-knockdown endothelial monolayers stained for F-actin and myosin-IIA. Scale bar, 50 μm. (B) Line scans across representative actin–myosin rings in control and WAVE2-depleted cells. (C) WAVE2 influences changes in circumferential actin rings and stress fibers induced by TNFα. Arrows indicate the circumferential to linear change in actin organization that results from TNFα. When WAVE2 is depleted, circumferential actin is increased and stress fibers are decreased with and without TNFα. Scale bar, 50 μm.

Antibodies to VE-cadherin included a monoclonal mouse anti–human CD144 antibody (clone 55-7H1; BD Biosciences, San Jose, CA) and a polyclonal rabbit anti–human VE-cadherin antibody (#2158; Cell Signaling, Danvers, MA). Anti-GFP was a rabbit polyclonal (ab6556; Abcam, Cambridge, MA). Anti-Arp3 was either a mouse anti–human monoclonal (FMS338; Sigma-Aldrich, St. Louis, MO) or a rabbit anti–bovine polyclonal (Welch *et al.*, 1997)). Rabbit anti–human WAVE-2 monoclonal antibody (D2C8, #3659) was from Cell Signaling. Mouse anti–human ZO-1 monoclonal antibody (ZO--1A12) was from Invitrogen (Camarillo, CA). Mouse anti–human glyceraldehyde-3-phosphate dehydrogenase monoclonal antibody (6C5) was from Abcam. Mouse anti–human vinculin monoclonal antibody (hVIN-1) was from Sigma-Aldrich. Rabbit anti–nonmuscle myosin heavy chain II-A polyclonal antibody (PRB-440P) was from Covance (Emeryville, CA). Secondary antibodies and phalloidin, fluorescently conjugated with Alexa dyes, were obtained from Molecular Probes (Life Technologies, Eugene, OR).

DNA and siRNAs

Human cDNA encoding WAVE2 fused at its C-terminus to GFP was a gift from Tadaomi Takenawa (Kobe University, Kobe, Japan). The WAVE2 coding region from that plasmid was subcloned into the

pBOB-GFP lentiviral vector (gift of George Bloom, University of Virginia, Charlottesville, VA). Lentivirus carrying the pBOB-GFP-WAVE2 plasmid were generated as described later. For expression of membrane-tagged GFP, plasmid 14757 was obtained from Addgene (Matsuda and Cepko, 2007).

siRNAs were obtained from Dharmacon (Thermo Scientific, Pittsburgh, PA). First, a pool of four siRNAs targeting human WAVE2 (ON-TARGETplus SMARTpools for WASF2) was tested to assess phenotype. Next individual siRNAs from that pool were tested. The oligonucleotide (GGAUUUGGGUCUCCAGGGA) that produced the largest decrease in WAVE2 expression (~80–85%, based on immunoblots; Supplemental Figure S1A) was chosen for subsequent studies. Off-target siRNA effects were excluded by demonstration of rescue of WAVE2-knockdown phenotypes by expression of WAVE2 from siRNA-resistant full-length cDNA constructs with six codon-neutral point mutations (GGcTTcGGcTCaCCgGGaA). Cells were transfected using Lipofectamine RNAiMAX transfection reagent (Invitrogen).

Lentivirus production

Human WAVE2-GFP and plain GFP, as a control, were expressed in HDMVECs by lentiviral transduction. Lentivirus was produced by transfecting a 6-cm dish of HEK293T cells with 4.8 µg of DNA, including pBOB-GFP (2 µg), pMDL/PRRE (1.45 µg), pVSVG (0.8 µg), and pRSV-rev (0.55 µg). Transfection was performed with TransIT-LT1 (Mirus, Madison, WI) in low-antibiotic HEK293T culture medium (DMEM, 10% FBS, 0.1× penicillin/streptomycin [pen/strep]). The medium was changed on the next day to DMEM with 30% FBS and 1× pen/strep. Media containing virus was collected 48 h posttransfection and concentrated by ultracentrifugation. For viral transduction, HDMVEC cells were incubated with lentivirus overnight in the presence of 10 µg/ml protamine sulfate.

Permeability assays

Permeability assays were performed by adding 40-kDa fluorescein isothiocyanate–dextran (gift from Robyn Klein, Washington University, St. Louis, MO) to the top chamber of a Transwell device. After 1 h, fluorescence was measure in medium collected from the bottom chamber. The permeability coefficient (PC) was calculated as follows:

$$\mathrm{PC} = \frac{V}{\mathrm{SA} \times C_D} \times \frac{C_R}{T}$$

In this equation, V is the volume of the receiving chamber, SA is the surface area, C_D is the concentration of tracer in the donor chamber at time zero, and C_R is the concentration of tracer in the receiving chamber at time T. C_R was calculated from fluorescence intensity. Permeability index was calculated by normalizing PC values on a scale from 0 to 1, with 0 defined as the value for control monolayers and 1 as the value for the Transwell membrane alone without ECs.

Staining of cells with fluorescent antibodies and phalloidin

In most cases, cells were fixed with paraformaldehyde, permeabilized, and incubated with primary and secondary antibodies as described (Mooren *et al.*, 2009). In some cases, the fixative was trichloroacetic acid (TCA); cells were treated with ice-cold 10% TCA for 15 min. Fluorescent phalloidin was added to secondary antibody solution in some cases. Coverslips were mounted in Vectashield (H1000; Vector Laboratories, Burlingame, CA) or ProLong Gold (Life Technologies, Grand Island, NY).

Light microscopy

For immunofluorescence, a set of *z*-stack images was collected with a laser-scanning confocal microscope (Zeiss 510 LSM; Zeiss, Jena, Germany) using a 40×/1.2 numerical aperture (NA) water immersion objective. Wide-field fluorescence images were collected using an inverted microscope (Olympus IX-81; Olympus, Center Valley, PA) with a 40×/0.75 NA objective, a Hg-lamp light source and a Hamamatsu electron-multiplying charge-coupled device video camera (Hamamatsu, Bridgewater, NJ).

Live-cell movies, with fluorescence and differential interference contrast (DIC) optics, were collected on a Zeiss 510 LSM equipped with a CO_2- and temperature-controlled stage insert (Tokai Hit, Shizuoka-ken, Japan). Movies were also collected on an inverted microscope (Olympus IX73) equipped with a CoolSnap HQ video camera (Photometrics, Tucson, AZ) and the same stage insert. Movies were collected with a 10×/0.25 NA phase objective or a 40×/0.75 NA objective.

Transwell assay for transmigration

HDMVECs were seeded at 3×10^4 cells/well in a 24-well Transwell dish (3-µm pore size; Corning, Fisher Scientific). Inserts were coated with 15 µg/ml fibronectin (Sigma-Aldrich) before seeding. Cells were cultured on Transwell for 48 h before experiments, with 20 ng/ml TNFα added for 4 h before addition of PBLs.

At time zero, TNFα-containing medium was removed from the Transwell chambers, 1.5×10^5 PBLs in regular HDMVEC medium were added to the top chamber, and medium with SDF1α (30 ng/ml) was added to the bottom chamber. PBLs were allowed to migrate across the Transwell at 37°C for 1 h. Cells were collected from the bottom chamber and counted using a hemocytometer.

Docking structure formation and staining

Anti-ICAM antibodies (rabbit or mouse, described earlier) were coupled to polystyrene beads (10 µm; Polysciences, Warrington, PA) per the manufacturer's recommendations. Anti-ICAM–coated beads were incubated with TNFα-treated HDMVECs (20 ng/ml TNFα, overnight) for 30 min at 37°C. To visualize the localization of F-actin and Arp2/3 complex to the anti-ICAM bead and docking structure, we stained cells with fluorescent phalloidin and antibodies, as described earlier. A *z*-series of images was collected with a laser-scanning confocal microscope (Zeiss LSM510). The images were scored for the presence of rings of F-actin or Arp2/3 complex around the beads.

In control experiments, beads coated with nonspecific anti–mouse or anti–rabbit immunoglobulin G did not adhere to TNFα-treated endothelial monolayers. In addition, the number of beads adhering to the cells and the number of docking structures were much less if ECs were not treated with TNFα, which increases the level of cell-surface ICAM-1 (Pober *et al.*, 1986; Dustin and Springer, 1988; Detmar *et al.*, 1990; Yang *et al.*, 2005).

Transendothelial resistance

HDMVECs were plated on fibronectin-coated Transwells as described and grown to confluence. Resistance across the Transwell filter was measured with an EVOM-2 m and an Endohm-6 electrode adapter (World Precision Instruments, Sarasota, FL). TER was calculated by subtracting the resistance of a blank well from that of the sample well and multiplying that difference by the surface area of the filter. The TER index was calculated by normalizing the TER values on a scale from 0 to 1, with 0 as the value for LatA treatment and 1 as the value for control monolayers.

Quantitation of the route of transmigration

HDMVECs were plated to confluence on fibronectin-coated polyacrylamide (PA) gels (Onken, Mooren, Mukherjee, Shahan, Li, and

Cooper, unpublished data. Coverslips were functionalized by silanization for 3 min using aminosilane (Sigma-Aldrich). Next the coverslips were treated for 30 min with 0.5% glutaraldehyde (Sigma-Aldrich). PA gels were made by using a mixture of 7% acrylamide and 3% (3-acrylamidopropyl) trimethylammonium chloride (Sigma-Aldrich) in phosphate-buffered saline. To vary the polymer stiffness, 0.4% bis-acrylamide was added. Next 0.1% APS (ammonium persulfate; Sigma-Aldrich) and 0.1% TEMED (*N*,*N*,*N*′,*N*′-tetramethylethylenediamine; Sigma-Aldrich) were added to the mixture to initiate polymerization. This gel mixture was placed as a large droplet on the functionalized coverslip. A nonfunctionalized glass coverslip was placed on top of the gel mixture to sandwich the liquid between the two coverslips to create a thin, flat gel. PA gels were polymerized for ~30 min before coating with fibronectin. Addition of 0.4% bis-acrylamide resulted in a ~50-kPa stiffness (Tse and Engler, 2010), which produced the highest number of transcellular-route migration events compared with glass and PA gels of higher or lower stiffness (Onken *et al*., unpublished data).

PBLs were added to confluent EC monolayers on PA gels for 15 min before fixation. Samples were processed for immunofluorescence and stained for VE-cadherin, ICAM-1, and F-actin in order to reveal the route of PBL transmigration. Events were counted by a variety of methods, but at least 15 fields of view were counted per dish. The percentage of cells was calculated by the total number of events divided by the total number of PBLs counted. The *p* values were calculated using a 2 × 2 contingency table and Fisher's exact test.

Quantitation of F-actin, myosin-IIA, and VE-cadherin

F-actin cytoskeletons were prepared from HDMVEC cells by treatment with 0.01% saponin and 0.07 μM phalloidin in 60 mM 1,4-piperazinediethanesulfonic acid, 25 mM 4-(2-hydroxyethyl)-1-piperazineethanesulfonic acid, 10 mM EGTA, and 2 mM $MgCl_2$, pH 6.9, for 3 min at 37°C. Cells were washed twice, and then hot 1× SDS sample buffer (50 mM Tris/HCl, pH 6.8, 4% SDS, 0.1% bromophenol blue, 10% glycerol, 5% β-mercaptoethanol) was added. SDS–PAGE and anti-actin immunoblots were performed. For myosin-IIA, corrected total cell fluorescence was calculated from immunofluorescence images as described (Burgess *et al*., 2010). For VE-cadherin, line scans with a width of 7 μm were prepared from representative portions of immunofluorescence images with ImageJ (National Institutes of Health, Bethesda, MD).

ACKNOWLEDGMENTS

We thank George Bloom and Tadaomi Takenawa for plasmids, Dorothy Schafer for stimulating discussions, and Dennis Oakley for assistance with the Zeiss 510 Laser Scanning Confocal in the Bakewell Neuroimaging Laboratory. The research was supported by National Institutes of Health Grants R01 GM 38542 to J.A.C. and F32 GM083538 to O.L.M. We used the cell-sorting service of the Flow Cytometry Core of the Alvin J. Siteman Cancer Center, which is supported in part by National Cancer Institute Grant P30 CA09184.

REFERENCES

Adams CL, Nelson WJ, Smith SJ (1996). Quantitative analysis of cadherin-catenin-actin reorganization during development of cell-cell adhesion. J Cell Biol 135, 1899–1911.

Aghajanian A, Wittchen ES, Allingham MJ, Garrett TA, Burridge K (2008). Endothelial cell junctions and the regulation of vascular permeability and leukocyte transmigration. J Thromb Haemost 6, 1453–1460.

Bakker W, Eringa EC, Sipkema P, van Hinsbergh VW (2009). Endothelial dysfunction and diabetes: roles of hyperglycemia, impaired insulin signaling and obesity. Cell Tissue Res 335, 165–189.

Barreiro O, Vicente-Manzanares M, Urzainqui A, Yanez-Mo M, Sanchez-Madrid F (2004). Interactive protrusive structures during leukocyte adhesion and transendothelial migration. Front Biosci 9, 1849–1863.

Barreiro O, Yanez-Mo M, Serrador JM, Montoya MC, Vicente-Manzanares M, Tejedor R, Furthmayr H, Sanchez-Madrid F (2002). Dynamic interaction of VCAM-1 and ICAM-1 with moesin and ezrin in a novel endothelial docking structure for adherent leukocytes. J Cell Biol 157, 1233–1245.

Bement WM, Forscher P, Mooseker MS (1993). A novel cytoskeletal structure involved in purse string wound closure and cell polarity maintenance. J Cell Biol 121, 565–578.

Bement WM, Mandato CA, Kirsch MN (1999). Wound-induced assembly and closure of an actomyosin purse string in Xenopus oocytes. Curr Biol 9, 579–587.

Blum MS, Toninelli E, Anderson JM, Balda MS, Zhou J, O'Donnell L, Pardi R, Bender JR (1997). Cytoskeletal rearrangement mediates human microvascular endothelial tight junction modulation by cytokines. Am J Physiol 273, H286–H294.

Bradfield PF, Scheiermann C, Nourshargh S, Ody C, Luscinskas FW, Rainger GE, Nash GB, Miljkovic-Licina M, Aurrand-Lions M, Imhof BA (2007). JAM-C regulates unidirectional monocyte transendothelial migration in inflammation. Blood 110, 2545–2555.

Bryce NS, Reynolds AB, Koleske AJ, Weaver AM (2013). WAVE2 regulates epithelial morphology and cadherin isoform switching through regulation of Twist and Abl. PLoS One 8, e64533.

Burgess A, Vigneron S, Brioudes E, Labbe JC, Lorca T, Castro A (2010). Loss of human Greatwall results in G2 arrest and multiple mitotic defects due to deregulation of the cyclin B-Cdc2/PP2A balance. Proc Natl Acad Sci USA 107, 12564–12569.

Campellone KG, Welch MD (2010). A nucleator arms race: cellular control of actin assembly. Nat Rev Mol Cell Biol 11, 237–251.

Carman CV, Jun CD, Salas A, Springer TA (2003). Endothelial cells proactively form microvilli-like membrane projections upon intercellular adhesion molecule 1 engagement of leukocyte LFA-1. J Immunol 171, 6135–6144.

Carman CV, Sage PT, Sciuto TE, de la Fuente MA, Geha RS, Ochs HD, Dvorak HF, Dvorak AM, Springer TA (2007). Transcellular diapedesis is initiated by invasive podosomes. Immunity 26, 784–797.

Carman CV, Springer TA (2004). A transmigratory cup in leukocyte diapedesis both through individual vascular endothelial cells and between them. J Cell Biol 167, 377–388.

Carman CV, Springer TA (2008). Trans-cellular migration: cell-cell contacts get intimate. Curr Opin Cell Biol 20, 533–540.

Cernuda-Morollon E, Gharbi S, Millan J (2010). Discriminating between the paracellular and transcellular routes of diapedesis. Methods Mol Biol 616, 69–82.

Clark PR, Manes TD, Pober JS, Kluger MS (2007). Increased ICAM-1 expression causes endothelial cell leakiness, cytoskeletal reorganization and junctional alterations. J Invest Dermatol 127, 762–774.

Daniel AE, van Buul JD (2013). Endothelial junction regulation: a prerequisite for leukocytes crossing the vessel wall. J Innate Immun 5, 324–335.

Dejana E, Orsenigo F, Lampugnani MG (2008). The role of adherens junctions and VE-cadherin in the control of vascular permeability. J Cell Sci 121, 2115–2122.

Derivery E, Gautreau A (2010). Generation of branched actin networks: assembly and regulation of the N-WASP and WAVE molecular machines. Bioessays 32, 119–131.

Detmar M, Imcke E, Ruszczak Z, Orfanos CE (1990). Effects of recombinant tumor necrosis factor-alpha on cultured microvascular endothelial cells derived from human dermis. J Invest Dermatol 95, 219S–222S.

Dustin ML, Springer TA (1988). Lymphocyte function-associated antigen-1. (LFA-1) interaction with intercellular adhesion molecule-1 (ICAM-1) is one of at least three mechanisms for lymphocyte adhesion to cultured endothelial cells. J Cell Biol 107, 321–331.

Helgeson LA, Nolen BJ (2013). Mechanism of synergistic activation of Arp2/3 complex by cortactin and N-WASP. Elife 2, e00884.

Heyraud S, Jaquinod M, Durmort C, Dambroise E, Concord E, Schaal JP, Huber P, Gulino-Debrac D (2008). Contribution of annexin 2 to the architecture of mature endothelial adherens junctions. Mol Cell Biol 28, 1657–1668.

Hoelzle MK, Svitkina T (2012). The cytoskeletal mechanisms of cell-cell junction formation in endothelial cells. Mol Biol Cell 23, 310–323.

Huveneers S, Oldenburg J, Spanjaard E, van der Krogt G, Grigoriev I, Akhmanova A, Rehmann H, de Rooij J (2012). Vinculin associates with endothelial VE-cadherin junctions to control force-dependent remodeling. J Cell Biol 196, 641–652.

Ibarra N, Pollitt A, Insall RH (2005). Regulation of actin assembly by SCAR/WAVE proteins. Biochem Soc Trans 33, 1243–1246.

Ivanov AI, Naydenov NG (2013). Dynamics and regulation of epithelial adherens junctions: recent discoveries and controversies. Int Rev Cell Mol Biol 303, 27–99.
Jacinto A, Martinez-Arias A, Martin P (2001). Mechanisms of epithelial fusion and repair. Nat Cell Biol 3, E117–E123.
Kumar P, Shen Q, Pivetti CD, Lee ES, Wu MH, Yuan SY (2009). Molecular mechanisms of endothelial hyperpermeability: implications in inflammation. Expert Rev Mol Med 11, e19.
Lou O, Alcaide P, Luscinskas FW, Muller WA (2007). CD99 is a key mediator of the transendothelial migration of neutrophils. J Immunol 178, 1136–1143.
Mamdouh Z, Mikhailov A, Muller WA (2009). Transcellular migration of leukocytes is mediated by the endothelial lateral border recycling compartment. J Exp Med 206, 2795–2808.
Martin P, Lewis J (1992). Actin cables and epidermal movement in embryonic wound healing. Nature 360, 179–183.
Martinelli R, Kamei M, Sage PT, Massol R, Varghese L, Sciuto T, Toporsian M, Dvorak AM, Kirchhausen T, Springer TA, Carman CV (2013). Release of cellular tension signals self-restorative ventral lamellipodia to heal barrier micro-wounds. J Cell Biol 201, 449–465.
Matsuda T, Cepko CL (2007). Controlled expression of transgenes introduced by in vivo electroporation. Proc Natl Acad Sci USA 104, 1027–1032.
Mattila PK, Lappalainen P (2008). Filopodia: molecular architecture and cellular functions. Nat Rev Mol Cell Biol 9, 446–454.
Mooren OL, Kotova TI, Moore AJ, Schafer DA (2009). Dynamin2 GTPase and cortactin remodel actin filaments. J Biol Chem 284, 23995–24005.
Muller WA (2009). Mechanisms of transendothelial migration of leukocytes. Circ Res 105, 223–230.
Muller WA, Weigl SA, Deng X, Phillips DM (1993). PECAM-1 is required for transendothelial migration of leukocytes. J Exp Med 178, 449–460.
Nourshargh S, Hordijk PL, Sixt M (2010). Breaching multiple barriers: leukocyte motility through venular walls and the interstitium. Nat Rev Mol Cell Biol 11, 366–378.
Nwariaku FE, Rothenbach P, Liu Z, Zhu X, Turnage RH, Terada LS (2003). Rho inhibition decreases TNF-induced endothelial MAPK activation and monolayer permeability. J Appl Physiol (1985) 95, 1889–1895.
Ostermann G, Weber KS, Zernecke A, Schroder A, Weber C (2002). JAM-1 is a ligand of the beta(2) integrin LFA-1 involved in transendothelial migration of leukocytes. Nat Immunol 3, 151–158.
Padrick SB, Doolittle LK, Brautigam CA, King DS, Rosen MK (2011). Arp2/3 complex is bound and activated by two WASP proteins. Proc Natl Acad Sci USA 108, E472–E479.
Pober JS, Gimbrone MAJ, Lapierre LA, Mendrick DL, Fiers W, Rothlein R, Springer TA (1986). Overlapping patterns of activation of human endothelial cells by interleukin 1, tumor necrosis factor, and immune interferon. J Immunol 137, 1893–1896.
Prasain N, Stevens T (2009). The actin cytoskeleton in endothelial cell phenotypes. Microvasc Res 77, 53–63.
Rigor RR, Shen Q, Pivetti CD, Wu MH, Yuan SY (2013). Myosin light chain kinase signaling in endothelial barrier dysfunction. Med Res Rev 33, 911–933.
Schenkel AR, Mamdouh Z, Chen X, Liebman RM, Muller WA (2002). CD99 plays a major role in the migration of monocytes through endothelial junctions. Nat Immunol 3, 143–150.
Sima AV, Stancu CS, Simionescu M (2009). Vascular endothelium in atherosclerosis. Cell Tissue Res 335, 191–203.
Sircar M, Bradfield PF, Aurrand-Lions M, Fish RJ, Alcaide P, Yang L, Newton G, Lamont D, Sehrawat S, Mayadas T, *et al.* (2007). Neutrophil transmigration under shear flow conditions in vitro is junctional adhesion molecule-C independent. J Immunol 178, 5879–5887.
Sonnemann KJ, Bement WM (2011). Wound repair: toward understanding and integration of single-cell and multicellular wound responses. Annu Rev Cell Dev Biol 27, 237–263.
Stolpen AH, Guinan EC, Fiers W, Pober JS (1986). Recombinant tumor necrosis factor and immune interferon act singly and in combination to reorganize human vascular endothelial cell monolayers. Am J Pathol 123, 16–24.
Taha AA, Taha M, Seebach J, Schnittler HJ (2014). ARP2/3-mediated junction-associated lamellipodia control VE-cadherin-based cell junction dynamics and maintain monolayer integrity. Mol Biol Cell 25, 245–256.
Ti SC, Jurgenson CT, Nolen BJ, Pollard TD (2011). Structural and biochemical characterization of two binding sites for nucleation-promoting factor WASp-VCA on Arp2/3 complex. Proc Natl Acad Sci USA 108, E463–E471.
Tilghman RW, Hoover RL (2002). The Src-cortactin pathway is required for clustering of E-selectin and ICAM-1 in endothelial cells. FASEB J 16, 1257–1259.
Tse JR, Engler AJ (2010). Preparation of hydrogel substrates with tunable mechanical properties. Curr Protoc Cell Biol Chapter 10, Unit 10.16.
van Buul JD, Allingham MJ, Samson T, Meller J, Boulter E, Garcia-Mata R, Burridge K (2007). RhoG regulates endothelial apical cup assembly downstream from ICAM1 engagement and is involved in leukocyte trans-endothelial migration. J Cell Biol 178, 1279–1293.
van Rijssel J, Kroon J, Hoogenboezem M, van Alphen FP, de Jong RJ, Kostadinova E, Geerts D, Hordijk PL, van Buul JD (2012). The Rho-guanine nucleotide exchange factor Trio controls leukocyte transendothelial migration by promoting docking structure formation. Mol Biol Cell 23, 2831–2844.
van Wetering S, van Buul JD, Quik S, Mul FP, Anthony EC, ten Klooster JP, Collard JG, Hordijk PL (2002). Reactive oxygen species mediate Rac-induced loss of cell-cell adhesion in primary human endothelial cells. J Cell Sci 115, 1837–1846.
van Wetering S, van den Berk N, van Buul JD, Mul FP, Lommerse I, Mous R, ten Klooster JP, Zwaginga JJ, Hordijk PL (2003). VCAM-1-mediated Rac signaling controls endothelial cell-cell contacts and leukocyte transmigration. Am J Physiol Cell Physiol 285, C343–C352.
Verma S, Han SP, Michael M, Gomez GA, Yang Z, Teasdale RD, Ratheesh A, Kovacs EM, Ali RG, Yap AS (2012). A WAVE2-Arp2/3 actin nucleator apparatus supports junctional tension at the epithelial zonula adherens. Mol Biol Cell 23, 4601–4610.
Weber C, Fraemohs L, Dejana E (2007). The role of junctional adhesion molecules in vascular inflammation. Nat Rev Immunol 7, 467–477.
Welch MD, Iwamatsu A, Mitchison TJ (1997). Actin polymerization is induced by Arp2/3 protein complex at the surface of Listeria monocytogenes. Nature 385, 265–269.
Wittchen ES (2009). Endothelial signaling in paracellular and transcellular leukocyte transmigration. Front Biosci 14, 2522–2545.
Wojciak-Stothard B, Entwistle A, Garg R, Ridley AJ (1998). Regulation of TNF-alpha-induced reorganization of the actin cytoskeleton and cell-cell junctions by Rho, Rac, and Cdc42 in human endothelial cells. J Cell Physiol 176, 150–165.
Wojciak-Stothard B, Ridley AJ (2002). Rho GTPases and the regulation of endothelial permeability. Vascul Pharmacol 39, 187–199.
Yamazaki D, Fujiwara T, Suetsugu S, Takenawa T (2005). A novel function of WAVE in lamellipodia: WAVE1 is required for stabilization of lamellipodial protrusions during cell spreading. Genes Cells 10, 381–392.
Yamazaki D, Oikawa T, Takenawa T (2007). Rac-WAVE-mediated actin reorganization is required for organization and maintenance of cell-cell adhesion. J Cell Sci 120, 86–100.
Yamazaki D, Suetsugu S, Miki H, Kataoka Y, Nishikawa S, Fujiwara T, Yoshida N, Takenawa T (2003). WAVE2 is required for directed cell migration and cardiovascular development. Nature 424, 452–456.
Yang L, Froio RM, Sciuto TE, Dvorak AM, Alon R, Luscinskas FW (2005). ICAM-1 regulates neutrophil adhesion and transcellular migration of TNF-alpha-activated vascular endothelium under flow. Blood 106, 584–592.
Yang L, Kowalski JR, Yacono P, Bajmoczi M, Shaw SK, Froio RM, Golan DE, Thomas SM, Luscinskas FW (2006a). Endothelial cell cortactin coordinates intercellular adhesion molecule-1 clustering and actin cytoskeleton remodeling during polymorphonuclear leukocyte adhesion and transmigration. J Immunol 177, 6440–6449.
Yang L, Kowalski JR, Zhan X, Thomas SM, Luscinskas FW (2006b). Endothelial cell cortactin phosphorylation by Src contributes to polymorphonuclear leukocyte transmigration in vitro. Circ Res 98, 394–402.
Yan C, Martinez-Quiles N, Eden S, Shibata T, Takeshima F, Shinkura R, Fujiwara Y, Bronson R, Snapper SB, Kirschner MW, *et al.* (2003). WAVE2 deficiency reveals distinct roles in embryogenesis and Rac-mediated actin-based motility. EMBO J 22, 3602–3612.